Analysis and Design of Marine Structures – Guedes Soares & Shenoi (Eds)

Corrosion fatigue crack growth in offshore wind monopile steel HAZ material

O. Adedipe, F. Brennan & A. Kolios
Cranfield University, Bedfordshire, UK

ABSTRACT: Offshore wind is an emerging clean and environmentally friendly renewable energy source that has developed rapidly to meet the European Union 2020 renewable energy targets. Monopiles are the most commonly used offshore wind turbine support structures and are exposed to harsh marine environments similar to those experienced by structures for oil and gas applications. However, they have significantly different design requirements due to operational loads envelope and structural stiffness. Therefore the knowledge of corrosion assisted fatigue damage in monopile support structures is of a vital importance to ensure economical and safe operation of the structures in service. In this paper, results are presented on fatigue crack growth of HAZ (Heat Affected Zone) specimens made of S355 J2+N steel in air and in free corrosion conditions. The fatigue crack response in the HAZ materials are compared to that of the base material and significant difference in the test results is discussed.

1 INTRODUCTION

The knowledge of corrosion assisted fatigue damage in offshore structures is of a vital importance to ensure economical and safe operation of the structures in service. Offshore wind turbines supported on monopile structures are exposed to harsh marine environments similar to that experienced by structures for Oil and Gas applications but they have significantly different design requirements due to operational loads envelope and structural stiffness. Fatigue cracks occur at the welded joints, in most cases at the Heat Affected Zones (HAZ) of these structures due to significant levels of local stress concentrations imposed by the geometry and effects of residual stresses introduced by welding process. The magnitude of the imposed welding residual stresses and the amount of change in the mechanical properties and microstructure of the HAZ depends on heating and cooling rates, material type, type of welding process and the level of restraint employed during the welding process.

Residual stress effects can also be considered as mean stresses, tensile residual stresses keep the crack open during propagation, while compressive residual stresses introduce crack closure effects which occur when the fatigue crack surface comes in contact during the unloading part of the applied cycle. During crack closure, the applied stress intensity factor range (ΔK) is significantly reduced to an effective stress intensity factor range (ΔK_{eff}) particularly at lower ΔK and lower stress ratios. This mechanism and its effect on fatigue crack growth can be corrected for by using the available crack closure models (Elber 1971, Schijve 1981, Kumar & Singh 1995) or by testing at higher stress ratios on the premise that larger part of fatigue life is consumed at such stress ratios.

Also, during crack propagation, residual stress is released progressively and eventually disappears. Therefore, its subsequent effect on fatigue crack growth is expected to occur at the early stages of crack propagation (Austin 1994). Austin also mentioned that, for welded plates, the tensile or damaging part of the residual stress field is about a quarter of the plate thickness such that the stress field is compressive in the middle of the plate owing to the self-equilibrating nature of a residual stress distribution. This implies that for tests conducted at higher stress ratios, the crack surface is fully open and the load range is completely effective during crack propagation. Therefore the effect of crack closure imposed by residual stress at higher levels of externally applied load is likely to disappear. As such, a conservative procedure for fatigue life calculations is to conduct experimental tests at higher stress ratio so that damaging or tensile residual stress are redistributed and their likely effect on fatigue crack propagation can be quantified by a mean stress approach.

Offshore wind turbines supported on monopile structures are the most commonly used support structures due to their simplicity in design. A significant number of corrosion fatigue studies have been conducted on offshore structural steels such as BS4360 50D steel for use in oil and gas applications

(Bardal & Haagensen 1977, Haagensen & Dagestad 1978, Thorpe et al. 1983, Scott et al. 1983). Some interesting results on the effect of mechanical loading and cathodic protection on C-Mn steel weldments with a yield strength of 490 MPa were also published by (Bertini 1991). Many of these studies have clearly demonstrated the damaging effect of seawater on fatigue crack growth irrespective of the applied levels of cathodic protection. However, there is still a deficit of information on free corrosion condition studies on offshore steel weldments in literature. The fact that a free corrosion condition is not design for in offshore structures does not guarantee it from occurring, coupled with unexpected situations due to likely loss of corrosion protection over time.

Hence, the existing corrosion fatigue database will therefore need to be updated so that this area of context can be properly addressed. Also the design for fatigue and corrosion assisted fatigue damage in oil and gas structures is primarily attributed to wave loads unlike the offshore wind structures which are exposed to wind/wave loads and wind-induced machine loads. As such, some of the available design concepts of offshore support structures are not likely to suit wind turbine supports design requirements. Some of the Oil and Gas structures design concepts might still be transferred to proposed jacket support structures for wind turbines in deeper water depths but careful consideration must be taken by design engineers in the aspects of loading and corrosion effects for such structures to be optimally designed.

Efforts have been made to study the structural dynamic response characteristics of wind turbines (Andersen et al. 2012, Lombardi et al. 2013, Bhattacharya et al. 2013). These studies have revealed that the support structure first-order structural dynamic response lies in the range of 0.3–0.4 Hz. This depends on a number of design factors such as water depth, monopile diameter and thickness, turbine size and soil conditions. With rapid development in the wind sector, there are possibilities of using larger wind turbines supported on thicker monopile structures in deep water depths with a view to increase their generating capacity. Therefore, such wind turbines are likely to have different dynamic response characteristics.

Corrosion fatigue is a complex phenomenon which cannot be completely understood due to the number of parameters involved in the process. However, the effect of loading frequency on the damage process is significant due to longer time the crack tip is exposed to the corrosion elements. Since fatigue cracks initiate at the HAZ of welded joints, the effect of corrosion on fatigue crack growth at that location of monopile support structures should be studied and better understood to ensure their fitness for purpose. This is demonstrated in this paper by conducting constant amplitude fatigue propagation tests in the HAZ of representative Compact Tension (CT) specimens in air and seawater environment similar to what might be experienced by real monopile support structures in service.

2 MATERIAL AND SPECIMEN PREPARATION

The material used for this experimental investigation was a 90 mm thick plate manufactured from EN10025-2:2004 S355 J2+N steel. The plate was welded with filler materials of similar composition to the base material and through a standard procedure similar to those used for monopile supports fabrications. The inside of the plate was welded first and subsequently welding layers were deposited on the outside to complete the process. 16 mm thick Compact Tension (CT) specimens with width W = 50 mm, designed in accordance with ASTM E647 (ASTM E647 2008) were extracted through the thickness of the plate with the notch perpendicular to the rolling direction of the plate. The specimen's starter notch was prepared by spark erosion and was positioned at the HAZ in order to reproduce the direction of crack growth in real monopiles. Specimens for characterization of the weld and the HAZ areas were taken from different locations of the plate along the thickness.

The specimens were then polished and etched to reveal the HAZ and weld area and to establish the uniformity of the HAZ dimensions over the entire length of the plate. Careful precautions were taken to substantiate that the HAZ is aligned with the crack path and to avoid possibilities of cracks growing into the parent material or the weld region. The extraction description is represented in Figure 1 indicating the HAZ location in the direction of the machined notch while the CT specimen design is depicted in Figure 2. The specimen surfaces were polished with emery papers of appropriate grits for adequate visual observation of the crack front.

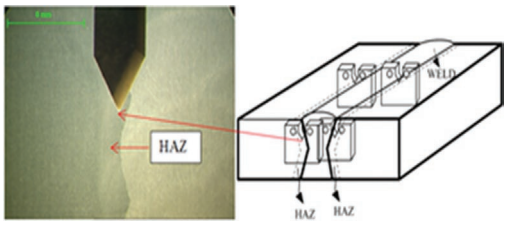

Figure 1. Compact Tension specimen's extraction.

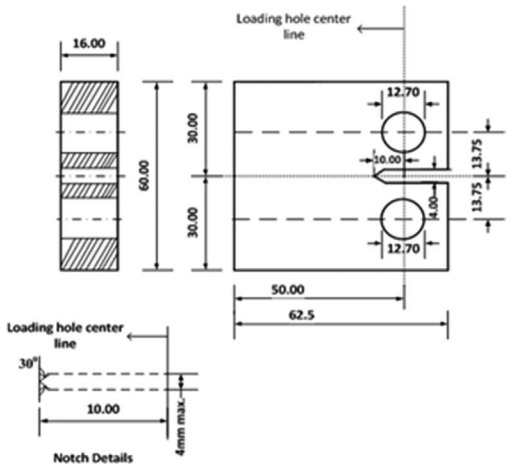

Figure 2. Compact Tension specimen design.

3 EXPERIMENTAL TESTS PROCEDURE

Fatigue crack propagation tests were carried out in accordance with ASTM E647 under load control on two 100 kN capacity servo—hydraulic machine with digital controllers. The specimens were precracked in air using the procedure recommended in ASTM E647. This is to ensure that both air and corrosion tests were carried out over a valid crack length that will minimize the effect of the plastic zone size associated with the notch. Tests were conducted using constant amplitude sinusoidal waveform at load ratio of 0.1 and loading frequencies of 2 to 5 Hz in air and at 0.3 Hz in artificial seawater. The artificial seawater used for corrosion fatigue tests was prepared according to specifications in ASTM D1141 (ASTM D1141 2008) and was circulated past the fully immersed specimens through a purpose designed corrosion rig at the rate of 3 litres per minute, at a temperature of 8–10 °C and at a pH of 7.78 to 8.2.

The artificial seawater temperature was monitored at the reservoir through a digital thermometer and at the corrosion chamber using an infrared thermometer with the probe positioned close to the notch tip in order to achieve the required water temperature at the crack tip. The entire corrosion system; the chamber, fittings, flow lines, reservoirs and the pumps are made of plastics to avoid the introduction of other metallic ions into the water. Tests were conducted on the HAZ specimens with the location of the notch tip aligned approximately in the middle of the HAZ.

Crack lengths were monitored using digital camera and Back Face Strain (BFS) methods. In the BFS method, a strain gauge was installed on the back face of each specimen to measure the strain values as the fatigue crack propagates. Optical measurements of crack lengths were performed in air to allow for calibration data for the back face strain measurements that were employed for the corrosion fatigue tests. The strain gauges were coated by four different layers of Neoprene rubber coating material to protect them from the effect of the corrosive environment over the entire test period. Crack growth rates (da/dN) were determined from the plots of crack lengths versus number of cycles using the seven point incremental polynomial method recommended in ASTM E647. This method is preferred over the secant method due to its ability to numerically smooth experimental data.

4 RESULTS AND DISCUSSION

Crack growth rates obtained in air and in the free corrosion condition are shown in Figure 3 to Figure 8 as plots of da/dN versus ΔK on logarithmic

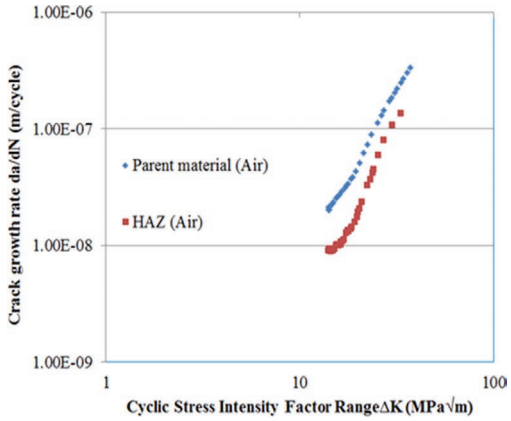

Figure 3. Comparison of crack growth rate in parent and HAZ materials in air.

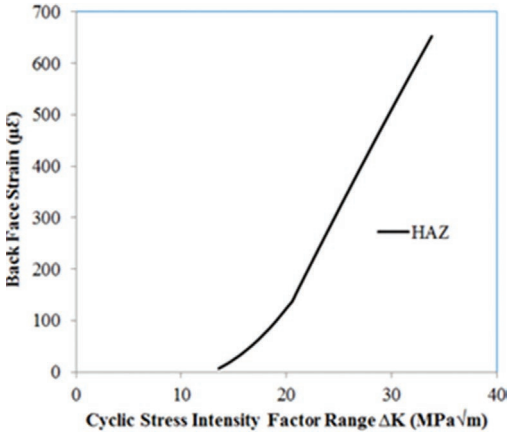

Figure 4. Closure effect due to residual stresses in HAZ.

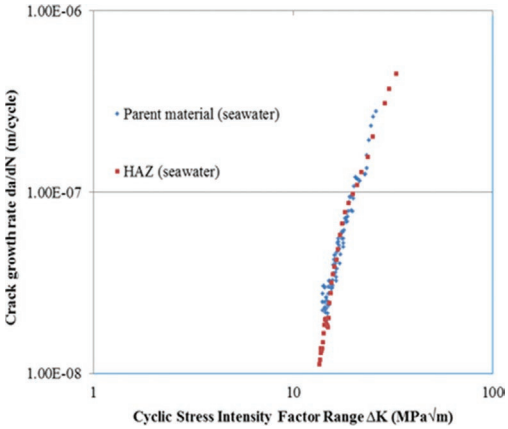

Figure 5. Comparison of crack growth rate in parent material and HAZ in free corrosion conditions.

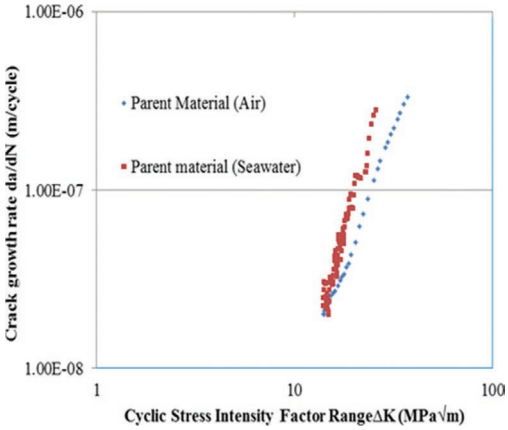

Figure 6. Comparison of crack growth rate in parent material in air and free corrosion conditions

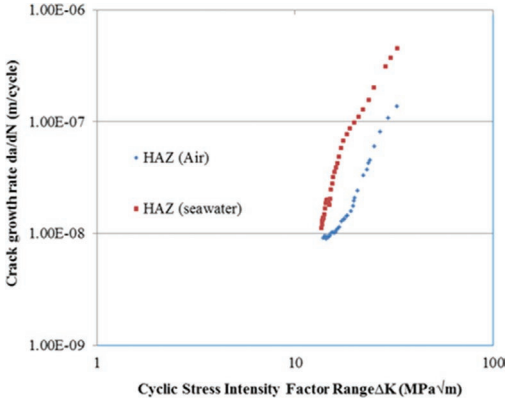

Figure 7. Crack growth rate in HAZ in air and free corrosion conditions.

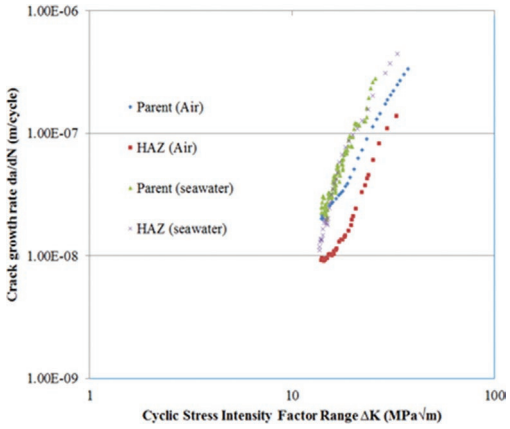

Figure 8. Crack growth rate in parent and HAZ materials in air and free corrosion conditions.

scales. All the analysed crack growth data correlates well with the Paris Law. Figure 3 compares crack growth rates in parent and HAZ material in air. At lower values of ΔK, the crack growth rates were found to be higher in parent material than in HAZ by approximately a factor of 4, but at higher ΔK, crack growth rates were observed to be approximately twice as fast in the parent material than in HAZ. A change in slope of the da/dN versus ΔK was also observed in the HAZ material as shown in Figure 3. This effect could be attributed to crack closure induced by mean or residual stresses. The effect can also be explained by the bilinear relationship and changes in slope of Back Face Strain versus ΔK as shown in Figure 4.

A similar phenomenon was also reported in a study of crack growth rate in C-Mn steel HAZ material (Beghini & Bertini 1990, Bertini 1991). Also, the likely effect of tensile residual stress close to the surface of the plate can be judged by a difference in the expended number cycles to crack initiation in the HAZ material which was approximately twice of that in the parent material.

Ideally, lower crack growth rates due to crack closure effects may lead to compressive stress cycle in fatigue crack propagation even if the nominal applied stress cycle is wholly tensile. In such situations, the applied ΔK is not affected but the effective R is increased or reduced depending on the magnitude of the stress and its location within the reference structure but this is not considered in this paper. Also, considering the effects of the welding sequence employed in preparing the plate and the nature of the HAZ crack growth curve in air at lower ΔK on the type of through-thickness crack growth that might be experienced by the circumferential weld regions of real monopiles, one can also say that the effect of the damaging portion of the

residual stress distribution that might be present in the welded area will affect crack growth close to the surface regardless of the crack initiation site(s) (either from inside or outside of the weld area) relative to the beneficial effect which will likely occur in the middle of the weld.

However, this type of effect was not observed in parent material tested under the same applied load. Also, the nature of crack growth behaviour obtained at lower ΔK in the HAZ material as shown in Figure 3 are the data points obtained at early stages of crack growth which coincides with the middle section of the plate where the specimen was extracted. As the crack deepens, the trend is similar to that obtained in parent material and the two curves almost converged. Judging from the orientation of the specimens within the plate, it is likely that the local tensile residual stress close to the advancing crack released during the precracking stage, such that the effect of this portion of the stress distribution is not likely to contribute to crack propagation at higher ΔK. This type of behaviour is similar to the explanations given by Austin (1994). Also, during the fatigue precracking, a slightly larger crack front and large plastic zone size was noted through optical observations with the digital camera at the early stage of crack growth but subsequently, a much smaller crack front was observed. This is probably due to the effects of tensile residual stresses present in the material and at the depth close to the surface of the plate.

Observations revealed that the crack growth trends in parent material is similar to those obtained from BS4360 50D steel parent material (Thorpe et al. 1983, Scott et al. 1983) while the HAZ material exhibited similar shape to that of C-Mn steel HAZ material with 490 MPa yield stress (Bertini 1991). However, the fatigue data obtained from C-Mn may not be truly representative of those reported in this paper primarily due to significant difference in yield stress and test conditions. Details can be found in (Bertini 1991). The crack growth rates in parent material and HAZ in free corrosion conditions are compared in Figure 5. At lower ΔK, crack growth rates in parent material were slightly higher than that in the HAZ specimens with the latter having a lower stress intensity factor threshold (ΔK_{th}).

The two curves also have similar crack growth trends but crack growth rates were higher in the parent material than in the HAZ across all the tested ranges of ΔK regardless of the similarity in the two curves. There is no clear evidence at the moment indicating any significant effect of residual stress in the HAZ seawater crack growth data compared to what was observed in air (Figure 3). Though this effect could still be present due to a difference in the number of cycles consumed in the HAZ specimen which was approximately twice that of parent material but the type of relationship plotted in Figure 4 was not evident in seawater.

Air and seawater results of parent and HAZ materials are depicted in Figures 6 and 7. At lower values of ΔK in the parent material, crack growth rates in air and seawater were similar but at higher ΔK crack growth rates were approximately four—times faster in seawater than in air. A different crack growth trend was observed in the HAZ material in air and in the free corrosion conditions when compared to the observed crack growth rates in parent material. A noticeable difference of twice the crack growth rates in air were observed in seawater for $\Delta K < 15$ MPa$\sqrt{m}$. This could be as a result of the deleterious action of the seawater on some likely defects present in the weld coupled with the effects of the precracked length, soaking time, and heterogeneous nature of weldments in terms of microstructure and mechanical properties.

At mid-way through the specimens, crack growth rates in seawater were nearly five—times higher than in air and at higher values of ΔK, crack growth rates were found to be four—times higher in seawater than in air. It can be seen (Figure 7) that the trends are similar compared to that of lower values of ΔK. Crack growth rates in parent and HAZ materials tested in both environments are compared in Figure 8. Parent material results i.e. air data generally lie between the seawater results and HAZ air data with the HAZ material having the slowest crack growth as shown. In previous studies, crack closure induced by compressive residual stress was suggested to be the reason for the crack growth behaviour particularly at lower values of ΔK (Beghini & Bertini 1990, Bertini 1991).

5 CONCLUSIONS

An experimental study of constant amplitude fatigue propagation on offshore wind monopile steels HAZ material was conducted in air and in laboratory simulated free corrosion conditions. The following conclusions can be drawn from the study:

1. Crack growth rates were relatively slower in the HAZ material tested in air at lower values of ΔK possibly due to crack closure induced by residual stresses. The effect was observed by a change in slope of Back Face Strain (BFS) versus ΔK.
2. Residual stress effect on fatigue crack growth is likely to occur at early stages of crack growth and disappears progressively at higher ΔK.

3. Crack growth rates were higher in parent material than in HAZ across all the applied ΔK tested in air. At higher values of ΔK, similar crack growth trends were observed in the both materials and the crack growth curves nearly converged into one another.
4. Crack growth rates in HAZ were similar to that in parent material in free corrosion conditions but the crack growth rates were found to be higher than the HAZ across all the applied stress intensity factor ranges tested.

ACKNOWLEDGEMENTS

The authors acknowledge the support of the Petroleum Technology Development Fund (PTDF), Nigeria who supports the PhD of Oyewole Adedipe.

REFERENCES

Andersen, L.V., Vahdatirad, M.J, Sichani, M.T. & Sørensen, J.D. 2012. Natural frequencies of wind turbines on monopile foundations in clayey soils—A probabilistic approach. *Comput. Geotech*., vol. 43, pp. 1–11.

ASTM D1141-98. 2008. Standard practice for the preparation of substitute ocean water.

ASTM E647-08. 2008. Standard test method for measurement of fatigue crack growth rates.

Austin, J.A. 1994. The role of corrosion fatigue crack growth mechanisms in predicting the fatigue life of offshore tubular joints. University College London.

Bardal, E. & Haagensen, P.J. 1977. Corrosion fatigue crack propagation tests on steels for offshore structures. *In Offshore Technology Conference*. pp. 381–385.

Beghini, M. & Bertini, L. 1990. Fatigue crack propagation through residual stress fields with closure phenomena. *Eng. Fract. Mech*., vol. 36, no. 3, pp. 379–387.

Bertini, L. 1991. Influence of seawater and residual stresses on fatigue crack growth in C-Mn steel weld joints. *Theor. Appl. Fract. Mech*., vol. 16, no. 2, pp. 135–144.

Bhattacharya, S., Nikitas, N., Garnsey, J., Alexander, N.A., Cox, J., Lombardi, D., Muir Wood, D. & Nash, D.F.T. 2013. Observed dynamic soil–structure interaction in scale testing of offshore wind turbine foundations. *Soil Dyn. Earthq. Eng*., vol. 54, pp. 47–60.

Elber, W. 1971. The significance of fatigue crack closure. In: Damage tolerance in aircraft structures. *ASTM STP 486*," Philadelphia.

Haagenseb, P. & Dagestad, V. 1978. Random load crack propagation in seawater in a medium—strength structural steel. *Paper 22 in European Offshore Steels research seminar*.

Kumar, R. & Singh, K. 1995. Influence of stress ratio on fatigue crack growth in mild steel. *Eng. Fract. Mech*., vol. 50, no. 3, pp. 377–384.

Lombardi, D., Bhattacharya, S. & Muir Wood, D. 2013. Dynamic soil–structure interaction of monopile supported wind turbines in cohesive soil, *Soil Dyn. Earthq. Eng*., vol. 49, pp. 165–180.

Schijve, J. 1981. Some formulas for the crack opening stress level. *Eng. Fract. Mech*., vol. 14, pp. 461–465.

Scott, P.M., Thorpe, T.W., & Silvester, D.R.V. 1983. Rate—determining process for corrosion fatigue crack growth in ferrite steels in seawater. *Corros. Sci*., vol. 23, no. 6, pp. 559–575.

Thorpe, T.W., Scott, P.M., Rance, A. & Silvester, D. 1983. Corrosion fatigue of BS 4360:50D structural steel in seawater. *Int. J. Fatigue*, vol. 5, no. 3, pp. 123–133.